

Quasar Outflows and Their Energetics: A Review of VLT/UVES Observations of SDSS J024221.87+004912.6

DOYEE BYUN ¹, NAHUM ARAV ¹ AND PATRICK B. HALL²

¹*Department of Physics, Virginia Tech, Blacksburg, VA 24061, USA*

²*Department of Physics and Astronomy, York University, Toronto, ON M3J 1P3, Canada*

ABSTRACT

VLT/UVES observations of the quasar SDSS J024221.87+004912.6 have been analyzed. Four absorption outflow systems are identified: a C IV BAL at $v \approx -18,000$ km s⁻¹, and three narrower low-ionization systems with centroid velocities ranging from -1200 to -3500 km s⁻¹. Two of the systems are energetic enough to contribute to AGN feedback, with one system reaching above 5% of the quasar’s Eddington luminosity. This system is also at a distance of 67 kpc away from the quasar, the farthest detected mini-BAL absorption outflow from its central source to date.

1. INTRODUCTION

Quasar absorption outflows are seen in a large fraction of quasar spectra ($\lesssim 40\%$), often detected via blueshifted absorption troughs in the rest frame of quasars (Hewett & Foltz 2003; Dai et al. 2008; Knigge et al. 2008). These outflows are often mentioned as likely candidates for producing AGN feedback (e.g., Silk & Rees 1998; Scannapieco & Oh 2004; Ciotti et al. 2009; Yuan et al. 2018; Vayner et al. 2021). According to theoretical models, outflow systems require a kinetic luminosity (\dot{E}_k) of at least $\sim 0.5\%$ (Hopkins & Elvis 2010) or $\sim 5\%$ (Scannapieco & Oh 2004) of the quasar’s Eddington luminosity (L_{Edd}) to contribute to AGN feedback. Outflow systems that fit these criteria have been found (e.g., Moe et al. 2009; Arav et al. 2013, 2020; Chamberlain et al. 2015; Xu et al. 2019, 2020a,b; Miller et al. 2020a,b).

The kinetic luminosity of a quasar’s outflow system is dependent on its distance from its central source (R), which we can find by measuring both the electron number density (n_e) and ionization parameter (U_H) (Borguet et al. 2012a). Our group and others have used this method to find the distances of outflow systems in the past (de Kool et al. 2001, 2002; Hamann et al. 2001; Gabel et al. 2005; Borguet et al. 2012a; Xu et al. 2018; Arav et al. 2020; Miller et al. 2020a; Byun et al. 2022). Using the ratios between excited and resonance state column densities of ionized species (N_{ion}) can lead us to a value of n_e (Arav et al. 2018). Recently, the R and \dot{E}_k values of outflow components have been found in the VLT/UVES spectrum of SDSS J024221.87+004912.6 (hereafter J0242+0049 Byun et al. 2022) and SDSS J235702.54-004824.0 (hereafter J2357-0048, Byun et al.

2022, under preparation). This paper reviews the analysis of J0242+0049 by Byun et al. (2022).

The analysis of the objects is based on data from the VLT/UVES Spectral Quasar Absorption Database (SQUAD) published by Murphy et al. (2019), containing the spectra of 475 quasars. Analysis of more SQUAD objects will be conducted in the future.

J0242+0049 shows signs of six absorption outflow systems, three of which are viable for our analysis. The viability is determined by the presence of excited state absorption lines such as those of Si II*, O I*, and Fe II*.

This paper is structured as follows. Section 2 discusses the observation of J0242+0049, as well as the data acquisition process. In Section 3, we present the process of finding n_e and U_H through measuring ionic column densities. Section 4 shows the results of the analysis, including the energetics parameters of the outflow systems. Section 5 provides a discussion of the results, and Section 6 summarizes and concludes the paper. For both of the analyses, we have adopted a cosmology of $h = 0.696$, $\Omega_m = 0.286$, and $\Omega_\Lambda = 0.714$ (Bennett et al. 2014), and used the Python astronomy package Astropy (Astropy Collaboration et al. 2013, 2018) for cosmological calculations.

2. OBSERVATION, DATA ACQUISITION, AND LINE IDENTIFICATION

The quasar J0242+0049 (J2000: RA=02:42:22, DEC=+00:49:12.6; $z=2.06$) (Pâris et al. 2018) was observed in September 5, 2005 with the VLT/UVES as part of the program 075.B-0190(A), with resolution $R \simeq 40,000$ and wavelength coverage from 3291 to 9300 Å (Hall et al. 2007). The spectral data was reduced and normalized by its continuum and emission by Murphy

et al. (2019) as part of their SQUAD database. Broad and narrow absorption lines have been found in the spectrum of J0242+0049 by Hall et al. (2007), which we identify here as NAL S1 at -1200 km s^{-1} ($\text{Ly } \alpha$ FWHM = 240 km s^{-1}), mini-BAL S2 at -1800 km s^{-1} (N V FWHM = 900 km s^{-1}), mini-BAL S3 at -3500 km s^{-1} (N V FWHM = 720 km s^{-1}), and BAL S4 at $-18,000 \text{ km s}^{-1}$, as shown in the full spectrum in Figure 1. Two more systems are identified by Chen et al. (2021), which we label as A and B. The focus of the analysis shown in the paper is on systems S1 – S3.

The outflows show absorption from low ionization species such as Si II, C II, and Fe II, as well as lines of Ly α , C IV, N V, P V, Mg II, Al II, and Al III. For the purpose of measuring the ionic column densities, we convert the normalized spectrum data from wavelength to velocity space via the systemic redshift of the quasar.

3. ANALYSIS

3.1. Ionic Column Density

To find the physical characteristics of the outflow systems, we first find the column densities of the observed ions (N_{ion}). The simplest method of measuring column densities is by assuming the apparent optical depth (AOD) of a uniformly covered homogeneous source, as demonstrated by Savage & Sembach (1991). The AOD method is used to find lower limits of N_{ion} for singlets or contaminated doublets, or upper limits when there are no discernible absorption troughs.

When there are multiple lines of the same ion and energy state, we can use the partial covering (PC) method, which assumes a homogeneous source partially covered by the outflow (Barlow et al. 1997; Arav et al. 1999a; Arav et al. 1999b), and solves for a velocity dependent covering factor (de Kool et al. 2002; Arav et al. 2005), to improve our measurements by taking phenomena such as non-black saturation into account (Edmonds et al. 2011; Borguet et al. 2012).

We choose integration ranges that cover visible absorption in the data, while minimizing the effects of blending and contamination. For instance, for Si IV, we use the blue line for S3 and the red line for S2. Si II* of S1 shows contamination due to an intervening absorption feature, so we use the measured column density as an upper limit for the sake of our analysis. C IV of S2 is heavily blended between the red and blue features, so we choose a velocity range in which the blue and red spectra do not overlap with each other in order to find a lower limit of the column density.

The errors in the column densities are propagated from the errors in the normalized flux from the data, binned along with the data into segments of $\Delta v = 10$

km s^{-1} for numerical integration. 20% error is added in quadrature for the column density values adopted for photoionization analysis to take into account the uncertainty in the modeled continuum level (Xu et al. 2018).

3.2. Photoionization Analysis

We use a grid of photoionization models created using the spectral synthesis code Cloudy (version c17.00) (Ferland et al. 2017), in order to find the Hydrogen column density (N_H) and ionization parameter (U_H) that best fit the measured ionic column densities, following the method of previous works (e.g., Xu et al. 2019; Miller et al. 2018, 2020a).

We use Cloudy to create a grid of simulated models that correspond to different N_H and U_H values, assuming solar metallicity, and the spectral energy distribution (SED) of quasar HE 0238-1904 (hereafter HE0238) (Arav et al. 2013). The N_H and U_H parameters determine the ionic column densities of each model, which we compare with the measured column densities measured in the previous section. The $\log N_H$ and $\log U_H$ values from this analysis are shown in Table 1, as well as in Figure 2.

3.3. Electron Number Density

The electron number density and, by extension, the distance of the outflow systems from the central source, can be found by determining the abundance ratios, measured via column densities, between excited and resonance states of low ionization species (Moe et al. 2009). We use the CHIANTI 9.0.1 Database (Dere et al. 1997; Dere et al. 2019) to model the relationship between the ratio of excited and resonance state ion abundances, and the electron number density, based on collisional excitation. We overlay this relation with the ratios based on the measured column densities, as shown in Figure 3. For this object, we use the ratios $N(\text{Si II}^*)/N(\text{Si II})$, $N(\text{C II}^*)/N(\text{C II})$, and $N(\text{Fe II}^*)/N(\text{Fe II})$, where $N(ion)$ is the column density of a particular ion.

For S3, we have an upper limit given by the C II ratio, and a measurement from the Si II ratio which agree with one another. Our measurements of Fe II are dominated by noise, and as such, are not included in the n_e measurement. Taking the ratio of $N(\text{Si II}^*)/N(\text{Si II})$, we find that $\log n_e = 3.3_{-0.4}^{+0.8} [\text{cm}^{-3}]$. S2 provides us a measurement from C II, and upper limits from Si II and Fe II. From the $N(\text{C II}^*)/N(\text{C II})$ ratio, we find $\log n_e = 0.25_{-0.2}^{+0.2} [\text{cm}^{-3}]$. S1 only gives us a lower limit from C II, as the Si II* is contaminated by an intervening line and cannot give us a reliable ratio between $N(\text{Si II}^*)$ and $N(\text{Si II})$. Thus, we get a lower limit for the electron number density, $\log n_e > 2.0_{-0.45} [\text{cm}^{-3}]$.

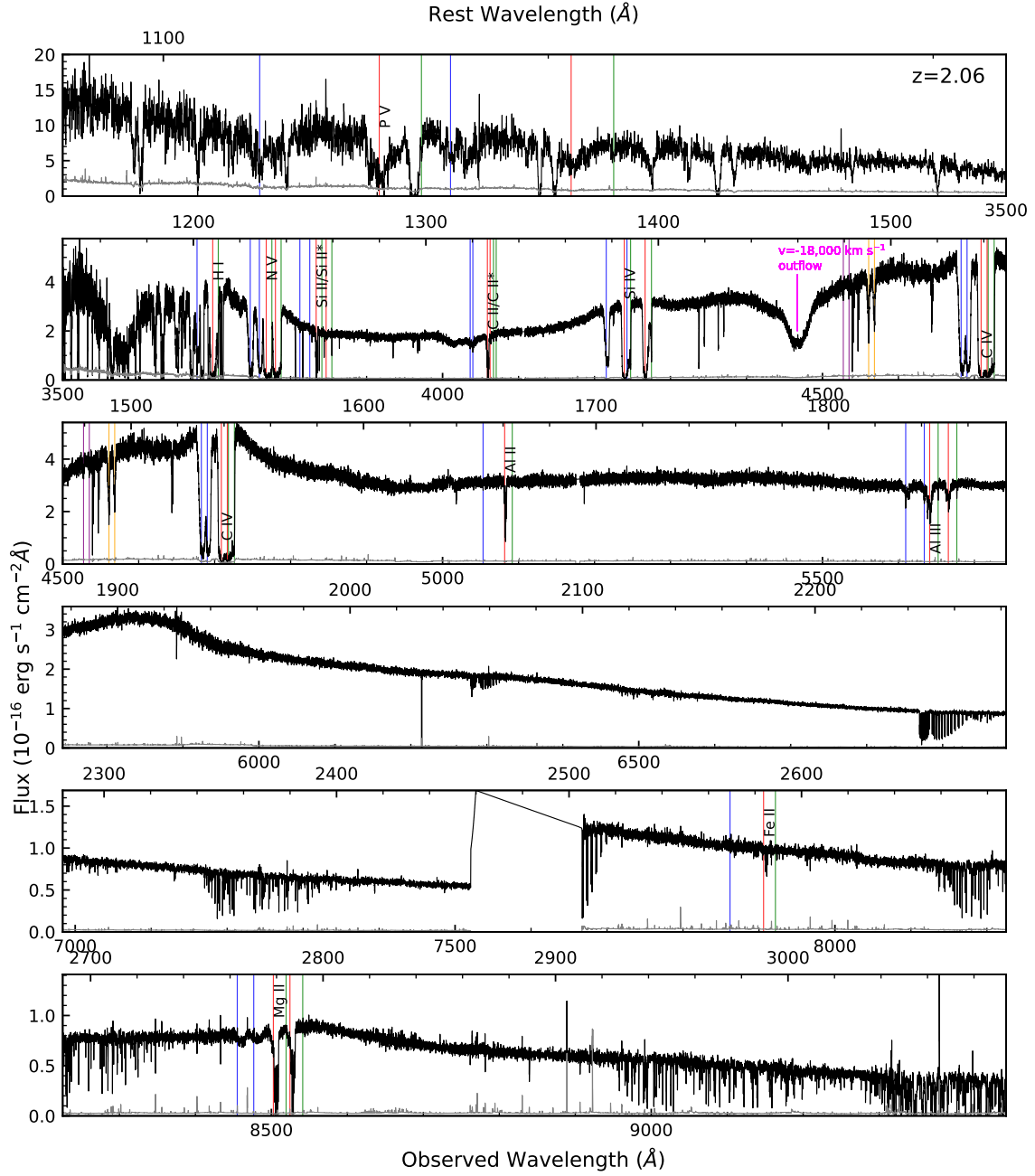


Figure 1. Normalized flux of J0242+0049 multiplied by the emission model by [Murphy et al. \(2019\)](#), based on the SQUAD data set. The flux has been scaled to match the BOSS spectrum from the epoch of MJD=57758 (Jan. 5, 2017) at observed wavelength $\lambda = 6500 \text{\AA}$. The black curve represents the flux, and the gray shows the error in flux. The green, red, and blue vertical lines mark absorption troughs of outflow systems S1, S2, and S3, respectively, while the S4 C IV BAL is labeled in magenta. Systems A and B are marked in orange and purple respectively. Note that the absorption troughs for S1 are significantly narrower when compared to those of S2 and S3.

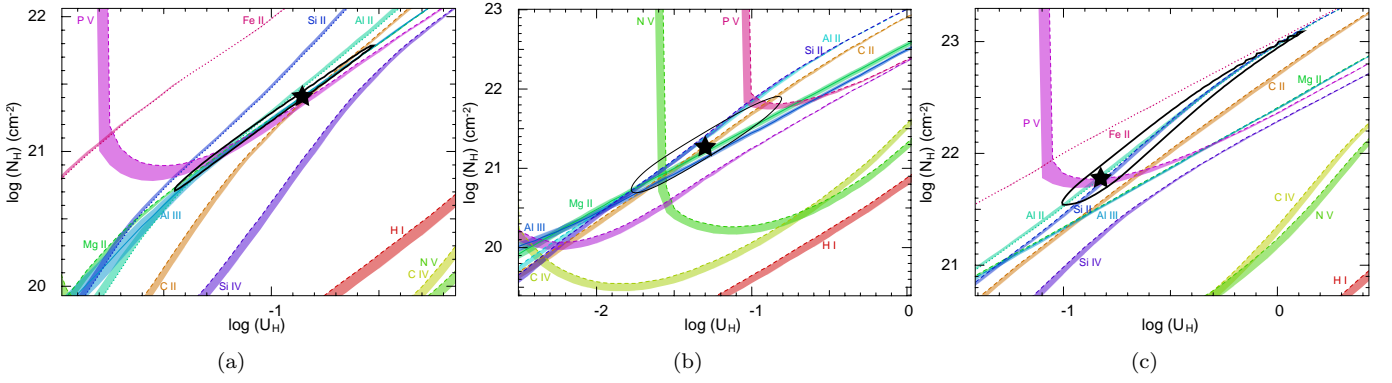


Figure 2. Plots of $\log N_H$ vs. $\log U_H$ for (a) S1, (b) S2, and (c) S3. The colored lines represent the N_H and U_H values allowed by the measured column densities of ions. Solid lines show measurements, dashed lines show lower limits, and dotted lines show upper limits. The colored bands attached to the lines represent the uncertainties in the column density measurements. The black stars in the plots show the solution for N_H and U_H found via χ^2 minimization, and the black ellipses represent the 1σ range for the solutions. For this calculation, the HE0238 SED and solar metallicity are assumed.

4. RESULTS

4.1. Distance and Kinetic Luminosity of the Outflows

In order to find the distance of the outflow systems, we use the definition for the ionization parameter

$$U_H \equiv \frac{Q_H}{4\pi R^2 n_H c} \quad (1)$$

where Q_H is the rate of ionizing photons, R is the distance of the outflow from the central source, and n_H is the hydrogen number density, which is estimated as $n_e \approx 1.2n_H$ for highly ionized plasma (Osterbrock & Ferland 2006). Since we have a solution for U_H from our photoionization analysis, as well as the n_e for each outflow from the excited to resonance state ratios, we can find R after determining the value of Q_H . We determined Q_H by first scaling the HE0238 SED to match the continuum flux at observed wavelength $\lambda = 6500 \text{ \AA}$ from the most recent SDSS observation ($F_\lambda = 1.4_{-0.14}^{+0.14} \times 10^{-16} \text{ erg s}^{-1} \text{ cm}^{-2} \text{ \AA}^{-1}$), and integrating over the scaled SED for energies above 1 Ryd, yielding $Q_H = 1.21_{-0.11}^{+0.11} \times 10^{57} \text{ s}^{-1}$. The corresponding $L_{bol} = 1.93_{-0.18}^{+0.18} \times 10^{47} \text{ erg s}^{-1}$ is larger than what would be expected from calculating the νL_ν at a specific wavelength via the method employed by Allen et al. (2011), as the HE0238 SED shows a large peak at the UV range ($\lambda \approx 1000 \text{ \AA}$, Arav et al. 2013). Applying a bolometric correction appropriate to 1700 \AA from Richards et al. (2006) brings the νL_ν reported by Allen et al. (2011) to within 20% of our calculated L_{bol} . The resulting outflow distances are shown in Table 1. Note that the distance of S2 (-1800 km s^{-1} , $R = 67_{-31}^{+55} \text{ kpc}$) is at least an order of magnitude larger than that of S3 (-3500 km s^{-1} , $R = 1.2_{-0.9}^{+0.8} \text{ kpc}$) or S1 (-1200 km s^{-1} , $R < 5.4_{-0.7}^{+7.3} \text{ kpc}$).

Once we have the distance of the outflow, we can find the mass flow rate (Borguet et al. 2012b)

$$\dot{M} \simeq 4\pi\Omega R N_H \mu m_p v \quad (2)$$

and the kinetic luminosity

$$\dot{E}_k \simeq \frac{1}{2} \dot{M} v^2 \quad (3)$$

assuming a partially filled shell, where Ω is the global covering factor (fraction of the total solid angle of the quasar that the outflow covers), $\mu = 1.4$ is the mean atomic mass per proton, m_p is the proton mass, and v is outflow velocity. For the global covering factor, we assume $\Omega = 0.2$, the portion of quasars from which C IV BALs are found (Hewett & Foltz 2003). As explained by Dunn et al. (2010), this is a reasonable assumption despite the relative rarity of quasars showing singly ionized absorption troughs such as Si II, due

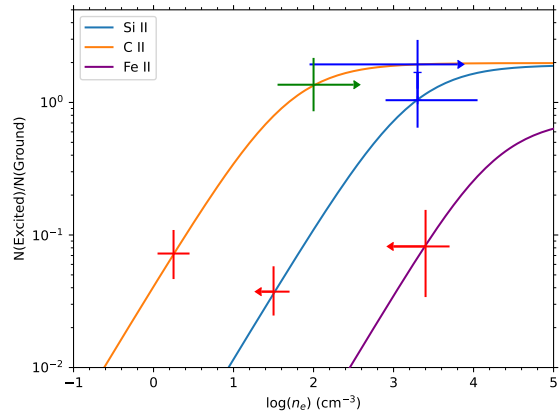


Figure 3. Ratio between excited and resonance state abundances of Si II, C II, and Fe II vs. $\log n_e$. The curves marked Si II, C II, and Fe II are the theoretical ratios modeled with CHIANTI, assuming a temperature of 10,000 K. The crosses on the curves show the ranges of the C II, Si II, and Fe II column density ratios, based on the measured AOD column densities. The green, red, and blue correspond to systems S1, S2, and S3 respectively. Arrows indicate either upper or lower limits in $\log n_e$ depending on the direction of the arrow. The upper limit of the $N(\text{Si II}^*)/N(\text{Si II})$ ratio for S3 is marked with a tick, as it overlaps with the error bars of the C II ratio of the same system.

to the likelihood that such quasars are regular BAL quasars seen from specific lines of sight. The resulting kinetic luminosity calculations yield $\log \dot{E}_K [\text{erg s}^{-1}] = 45.42_{-0.64}^{+1.33}$, $45.82_{-0.32}^{+0.37}$ for S3 and S2 respectively, as well as an upper limit of $\log \dot{E}_K < 44.33_{-0.61}^{+0.53}$ for S1. In addition, we calculate the momentum flux ($\dot{M}v$) of each outflow system (see Table 1) and compare it to the single-scattering limit of the quasar ($\frac{L_{bol}}{c} = 6.44_{-0.61}^{+0.61} \times 10^{36} \text{ erg cm}^{-1}$). The single-scattering limit assumes the scenario in which absorption of photon momentum drives acceleration (Abbott 1982; Arav & Li 1994). The momentum flux of S1 is smaller than the single-scattering limit, while those of S2 and S3 are above the limit. As S2 has a momentum flux an order of magnitude higher than the single-scattering limit, this implies the possibility of a multiple-scattering scenario (Lucy & Abbott 1993).

5. DISCUSSION

5.1. AGN Feedback Contribution of Outflows

As previously mentioned in the introduction, the kinetic luminosity (\dot{E}_k) of the outflow systems must be at least $\sim 0.5\%$ (Hopkins & Elvis 2010) or $\sim 5\%$ (Scannapieco & Oh 2004) of the source quasar's Eddington luminosity (L_{Edd}) to contribute to AGN feedback. In order to find this ratio, we must first find the Edding-

Table 1. Physical Properties J0242+0049 Outflow Systems

Outflow System	S1 = -1200 km s^{-1}	S2 = -1800 km s^{-1}	S3 = -3500 km s^{-1}
$\log(N_{\text{H}})$ [cm^{-2}]	$21.41^{+0.38}_{-0.70}$	$21.27^{+0.64}_{-0.58}$	$21.78^{+1.30}_{-0.24}$
$\log(U_{\text{H}})$ [dex]	$-0.86^{+0.33}_{-0.59}$	$-1.30^{+0.49}_{-0.48}$	$-0.83^{+0.95}_{-0.18}$
$\log(n_{\text{e}})$ [cm^{-3}]	$> 2.00_{-0.45}$	$0.25^{+0.20}_{-0.20}$	$3.30^{+0.75}_{-0.40}$
Distance [kpc]	$< 5.4^{+7.3}$	67^{+55}_{-31}	$1.2^{+0.8}_{-0.9}$
\dot{M} [$M_{\odot} \text{yr}^{-1}$]	$< 480^{+300}$	6500^{+8900}_{-3400}	700^{+2900}_{-30}
$\dot{M}v$ [$10^{36} \text{ erg cm}^{-1}$]	$< 3.6^{+2.3}$	74^{+100}_{-39}	$16^{+60}_{-0.7}$
$\log(\dot{E}_K)$ [erg s^{-1}]	$< 44.33^{+0.21}$	$45.82^{+0.37}_{-0.32}$	$45.43^{+0.7}_{-0.02}$
\dot{E}_K/L_{edd} [%]	$< 0.18^{+0.16}$	$5.5^{+8.8}_{-3.1}$	$2.3^{+9.9}_{-0.8}$

NOTE—Temperature of 10,000K assumed.

ton luminosity. We compute the mass of the black hole using the Mg II-based mass equation in Bahk et al. (2019), with the FWHM of the Mg II emission feature in the SDSS spectrum. To account for the Fe II emission throughout the spectrum, we use the Fe II template by Tsuzuki et al. (2006), and run a best fit algorithm to match the features in the spectrum, as done by Woo et al. (2018). This yields a black hole mass of $M_{\text{BH}} = 9.7^{+4.9}_{-3.4} \times 10^8 M_{\odot}$, corresponding to an Eddington luminosity of $L_{\text{Edd}} = 1.2^{+0.6}_{-0.4} \times 10^{47} \text{ erg s}^{-1}$. We expect the Fe II emission’s effect on the absorption to be small, as the fitted emission template from Tsuzuki et al. (2006) is $< 20\%$ of the continuum level of the SDSS spectrum of MJD=57758, leaving us with column densities that agree with our measured values within error.

Taking the ratio between the kinetic luminosity of each outflow system and the Eddington luminosity of the quasar, we find that S2 and S3 are well above the 0.5% threshold from Hopkins & Elvis (2010), and S2 is above the 5% threshold by Scannapieco & Oh (2004), while S1’s kinetic luminosity is below 0.18 % of the Eddington luminosity, as seen in Table 1. We can thus conclude that S2 and S3 are energetic enough to contribute to AGN feedback.

Unlike in objects analyzed in other papers (e.g. Miller et al. 2020a; Xu et al. 2020a), we do not have lines from the very high ionization phase. Thus, while there may

be a very high ionization phase, we cannot tell from the information we have.

5.2. SED and Metallicity Dependency, and Attenuation of the SED

An alternative to using the SED of HE 0238-1904 would be to use the theoretical SED as defined by Mathews & Ferland (1987), which is based on the He II line. The HE 0238-1904 SED is based on observation of a high quality spectrum which stretches into the far UV range, better representing a quasar spectrum (Arav et al. 2013). Just like in other objects(e.g. Xu et al. 2018; Miller et al. 2020a), higher metallicity drops the values of the energetics parameters. For instance, raising the metallicity to 4 times solar metallicity, using abundance ratios from Ballero et al. (2008), changes the photoionization solution of S2 to $\log U_{\text{H}} = -1.5^{+0.3}_{-0.3}$, and $\log N_{\text{H}} = 20.5^{+0.4}_{-0.4} [\text{cm}^{-2}]$, lowering the mass flow rate and kinetic luminosity to $\dot{M} = 1300^{+600}_{-400} M_{\odot} \text{yr}^{-1}$ and $\log \dot{E}_K = 45.13^{+0.17}_{-0.18} [\text{erg s}^{-1}]$ respectively. Using the SED by Mathews & Ferland (1987) with solar metallicity changes the solution to $\log U_{\text{H}} = -1.5^{+0.4}_{-0.4}$, $\log N_{\text{H}} = 21.2^{+0.5}_{-0.5}$, which is in agreement with the values in Table 1 within error.

It is possible that the SED seen by one outflow system can be attenuated by another, resulting in a smaller Q_{H} , and by extension, a smaller distance R . In particular, as

S2 is further out than the other mini-BAL system S3, it is likely that the SED seen by S2 is obscured by S3 (e.g., Bautista et al. 2010; Sun et al. 2017; Miller et al. 2018, 2020c). We used the method described by Miller et al. (2018) to test the effects of attenuation by S3. We used Cloudy to model the attenuated SED by S3 by inputting the relevant N_H and U_H values of S3 shown in Table 1. We then use that attenuated SED to find the resulting Q_H and R of S2. The reduced values for the parameters are $Q_H = 4.9_{-0.5}^{+0.5} \times 10^{56} \text{ s}^{-1}$ and $R = 43_{-20}^{+35} \text{ kpc}$, which is a $\sim 30\%$ decrease in the distance of S2. We choose S3 as the attenuation source, as its stronger features compared to S1 suggest that the attenuation effect from S3 would be larger than that of S1. We are unable to calculate the attenuation by S4, as we cannot obtain N_H or U_H from its singular C IV absorption trough.

6. SUMMARY AND CONCLUSION

This paper has presented the analysis of three absorption systems of quasar SDSS J0242+0049, dubbed S1, S2, and S3, from VLT/UVES observational data, as well as the velocity shift of the S4 C IV BAL across five different epochs. From the absorption troughs we identified, we measured the column densities of 11 ions in each system. Through photoionization analysis using the measured column densities, we found the best fit solutions to U_H and N_H for each system.

The abundance ratios between the excited and resonance states of ions Si II and C II were used to find the electron number density n_e of the three systems S1, S2, and S3, as shown in Figure 3. Equations 1, 2, and 3 used to find the distance from the central source, the mass flow rate, and the kinetic luminosity of each system respectively. The ratios between the kinetic luminosities and the quasar’s Eddington luminosity were found in order to evaluate their AGN feedback contribution, the results of which can be seen in Table 1. From this analysis, we have found that S2 and S3 have sufficient kinetic luminosity for AGN feedback contribution. Most notable in this result is the distance of S2 $R = 67 \text{ kpc}$, further than the absorption system of 3C 191 found at $R = 28 \text{ kpc}$ by Hamann et al. (2001), making this the furthest reported distance of a mini-BAL absorption outflow from its central source.

Through further observation and analysis, we expect to shed more light on the time variability of the S4 C IV BAL, as well as that of systems S1, S2, and S3.

NA and DB acknowledge support from NSF grant AST 2106249, as well as NASA STScI grants GO 14777, 14242, 14054, 14176, and AR-15786. DB acknowledges support from the Virginia Space Grant Consortium Graduate Research Fellowship Program.

REFERENCES

- Abbott, D. C. 1982, ApJ, 259, 282, doi: [10.1086/160166](https://doi.org/10.1086/160166)
- Allen, J. T., Hewett, P. C., Maddox, N., Richards, G. T., & Belokurov, V. 2011, MNRAS, 410, 860, doi: [10.1111/j.1365-2966.2010.17489.x](https://doi.org/10.1111/j.1365-2966.2010.17489.x)
- Arav, N., Becker, R. H., Laurent-Muehleisen, S. A., et al. 1999a, ApJ, 524, 566, doi: [10.1086/307841](https://doi.org/10.1086/307841)
- Arav, N., Borguet, B., Chamberlain, C., Edmonds, D., & Danforth, C. 2013, MNRAS, 436, 3286, doi: [10.1093/mnras/stt1812](https://doi.org/10.1093/mnras/stt1812)
- Arav, N., Kaastra, J., Kriss, G. A., et al. 2005, ApJ, 620, 665, doi: [10.1086/425560](https://doi.org/10.1086/425560)
- Arav, N., Korista, K. T., de Kool, M., Junkkarinen, V. T., & Begelman, M. C. 1999b, ApJ, 516, 27, doi: [10.1086/307073](https://doi.org/10.1086/307073)
- Arav, N., & Li, Z.-Y. 1994, ApJ, 427, 700, doi: [10.1086/174177](https://doi.org/10.1086/174177)
- Arav, N., Liu, G., Xu, X., et al. 2018, ApJ, 857, 60, doi: [10.3847/1538-4357/aab494](https://doi.org/10.3847/1538-4357/aab494)
- Arav, N., Xu, X., Miller, T., Kriss, G. A., & Plesha, R. 2020, ApJS, 247, 37, doi: [10.3847/1538-4365/ab66af](https://doi.org/10.3847/1538-4365/ab66af)
- Astropy Collaboration, Robitaille, T. P., Tollerud, E. J., et al. 2013, A&A, 558, A33, doi: [10.1051/0004-6361/201322068](https://doi.org/10.1051/0004-6361/201322068)
- Astropy Collaboration, Price-Whelan, A. M., Sipőcz, B. M., et al. 2018, AJ, 156, 123, doi: [10.3847/1538-3881/aabc4f](https://doi.org/10.3847/1538-3881/aabc4f)
- Bahk, H., Woo, J.-H., & Park, D. 2019, ApJ, 875, 50, doi: [10.3847/1538-4357/ab100d](https://doi.org/10.3847/1538-4357/ab100d)
- Ballero, S. K., Matteucci, F., Ciotti, L., Calura, F., & Padovani, P. 2008, A&A, 478, 335, doi: [10.1051/0004-6361:20078663](https://doi.org/10.1051/0004-6361:20078663)
- Barlow, T. A., Hamann, F., & Sargent, W. L. W. 1997, in Astronomical Society of the Pacific Conference Series, Vol. 128, Mass Ejection from Active Galactic Nuclei, ed. N. Arav, I. Shlosman, & R. J. Weymann, 13. <https://arxiv.org/abs/astro-ph/9705048>
- Bautista, M. A., Dunn, J. P., Arav, N., et al. 2010, ApJ, 713, 25, doi: [10.1088/0004-637X/713/1/25](https://doi.org/10.1088/0004-637X/713/1/25)
- Bennett, C. L., Larson, D., Weiland, J. L., & Hinshaw, G. 2014, ApJ, 794, 135, doi: [10.1088/0004-637x/794/2/135](https://doi.org/10.1088/0004-637x/794/2/135)

- Borguet, B., Edmonds, D., Arav, N., Dunn, J., & Kriss, G. A. 2012, *ApJ*, 751, 107, doi: [10.1088/0004-637X/751/2/107](https://doi.org/10.1088/0004-637X/751/2/107)
- Borguet, B. C. J., Edmonds, D., Arav, N., Benn, C., & Chamberlain, C. 2012a, *ApJ*, 758, 69, doi: [10.1088/0004-637X/758/1/69](https://doi.org/10.1088/0004-637X/758/1/69)
- Borguet, B. C. J., Edmonds, D., Arav, N., Dunn, J., & Kriss, G. A. 2012b, *ApJ*, 751, 107, doi: [10.1088/0004-637X/751/2/107](https://doi.org/10.1088/0004-637X/751/2/107)
- Byun, D., Arav, N., & Hall, P. B. 2022, *ApJ*, 927, 176, doi: [10.3847/1538-4357/ac503d](https://doi.org/10.3847/1538-4357/ac503d)
- Chamberlain, C., Arav, N., & Benn, C. 2015, *MNRAS*, 450, 1085, doi: [10.1093/mnras/stv572](https://doi.org/10.1093/mnras/stv572)
- Chen, C., Hamann, F., Ma, B., & Murphy, M. 2021, *ApJ*, 907, 84, doi: [10.3847/1538-4357/abcec5](https://doi.org/10.3847/1538-4357/abcec5)
- Ciotti, L., Ostriker, J. P., & Proga, D. 2009, *ApJ*, 699, 89, doi: [10.1088/0004-637X/699/1/89](https://doi.org/10.1088/0004-637X/699/1/89)
- Dai, X., Shankar, F., & Sivakoff, G. R. 2008, *ApJ*, 672, 108, doi: [10.1086/523688](https://doi.org/10.1086/523688)
- de Kool, M., Arav, N., Becker, R. H., et al. 2001, *ApJ*, 548, 609, doi: [10.1086/318996](https://doi.org/10.1086/318996)
- de Kool, M., Becker, R. H., Gregg, M. D., White, R. L., & Arav, N. 2002, *ApJ*, 567, 58, doi: [10.1086/338490](https://doi.org/10.1086/338490)
- de Kool, M., Korista, K. T., & Arav, N. 2002, *ApJ*, 580, 54, doi: [10.1086/343107](https://doi.org/10.1086/343107)
- Dere, K. P., Landi, E., Mason, H. E., Monsignori Fossi, B. C., & Young, P. R. 1997, *A&AS*, 125, 149, doi: [10.1051/aas:1997368](https://doi.org/10.1051/aas:1997368)
- Dere, K. P., Zanna, G. D., Young, P. R., Landi, E., & Sutherland, R. S. 2019, *ApJS*, 241, 22, doi: [10.3847/1538-4365/ab05cf](https://doi.org/10.3847/1538-4365/ab05cf)
- Dunn, J. P., Bautista, M., Arav, N., et al. 2010, *ApJ*, 709, 611, doi: [10.1088/0004-637X/709/2/611](https://doi.org/10.1088/0004-637X/709/2/611)
- Edmonds, D., Borguet, B., Arav, N., et al. 2011, *ApJ*, 739, 7, doi: [10.1088/0004-637X/739/1/7](https://doi.org/10.1088/0004-637X/739/1/7)
- Ferland, G. J., Chatzikos, M., Guzmán, F., et al. 2017, *RMxAA*, 53, 385. <https://arxiv.org/abs/1705.10877>
- Gabel, J. R., Kraemer, S. B., Crenshaw, D. M., et al. 2005, *ApJ*, 631, 741, doi: [10.1086/432682](https://doi.org/10.1086/432682)
- Hall, P. B., Sadavoy, S. I., Hutsemekers, D., Everett, J. E., & Rafée, A. 2007, *ApJ*, 665, 174, doi: [10.1086/519273](https://doi.org/10.1086/519273)
- Hamann, F. W., Barlow, T. A., Chaffee, F. C., Foltz, C. B., & Weymann, R. J. 2001, *ApJ*, 550, 142, doi: [10.1086/319733](https://doi.org/10.1086/319733)
- Hewett, P. C., & Foltz, C. B. 2003, *AJ*, 125, 1784, doi: [10.1086/368392](https://doi.org/10.1086/368392)
- Hopkins, P. F., & Elvis, M. 2010, *MNRAS*, 401, 7, doi: [10.1111/j.1365-2966.2009.15643.x](https://doi.org/10.1111/j.1365-2966.2009.15643.x)
- Knigge, C., Scaringi, S., Goad, M. R., & Cottis, C. E. 2008, *MNRAS*, 386, 1426, doi: [10.1111/j.1365-2966.2008.13081.x](https://doi.org/10.1111/j.1365-2966.2008.13081.x)
- Lucy, L. B., & Abbott, D. C. 1993, *ApJ*, 405, 738, doi: [10.1086/172402](https://doi.org/10.1086/172402)
- Mathews, W. G., & Ferland, G. J. 1987, *ApJ*, 323, 456, doi: [10.1086/165843](https://doi.org/10.1086/165843)
- Miller, T. R., Arav, N., Xu, X., Kriss, G. A., & Plesha, R. J. 2020a, *ApJS*, 247, 39, doi: [10.3847/1538-4365/ab5967](https://doi.org/10.3847/1538-4365/ab5967)
- . 2020b, *ApJS*, 249, 15, doi: [10.3847/1538-4365/ab94b9](https://doi.org/10.3847/1538-4365/ab94b9)
- . 2020c, *ApJS*, 247, 41, doi: [10.3847/1538-4365/ab5969](https://doi.org/10.3847/1538-4365/ab5969)
- Miller, T. R., Arav, N., Xu, X., et al. 2018, *ApJ*, 865, 90, doi: [10.3847/1538-4357/aad817](https://doi.org/10.3847/1538-4357/aad817)
- Moe, M., Arav, N., Bautista, M. A., & Korista, K. T. 2009, *ApJ*, 706, 525, doi: [10.1088/0004-637X/706/1/525](https://doi.org/10.1088/0004-637X/706/1/525)
- Murphy, M. T., Kacprzak, G. G., Savorgnan, G. A., & Carswell, R. F. 2019, *MNRAS*, 482, 3458, doi: [10.1093/mnras/sty2834](https://doi.org/10.1093/mnras/sty2834)
- Osterbrock, D. E., & Ferland, G. J. 2006, *Astrophysics of gaseous nebulae and active galactic nuclei*
- Pâris, I., Petitjean, P., Aubourg, É., et al. 2018, *A&A*, 613, A51, doi: [10.1051/0004-6361/201732445](https://doi.org/10.1051/0004-6361/201732445)
- Richards, G. T., Lacy, M., Storrie-Lombardi, L. J., et al. 2006, *ApJS*, 166, 470, doi: [10.1086/506525](https://doi.org/10.1086/506525)
- Savage, B. D., & Sembach, K. R. 1991, *ApJ*, 379, 245, doi: [10.1086/170498](https://doi.org/10.1086/170498)
- Scannapieco, E., & Oh, S. P. 2004, *ApJ*, 608, 62, doi: [10.1086/386542](https://doi.org/10.1086/386542)
- Silk, J., & Rees, M. J. 1998, *A&A*, 331, L1. <https://arxiv.org/abs/astro-ph/9801013>
- Sun, L., Zhou, H., Ji, T., et al. 2017, *ApJ*, 838, 88, doi: [10.3847/1538-4357/aa63eb](https://doi.org/10.3847/1538-4357/aa63eb)
- Tsuzuki, Y., Kawara, K., Yoshii, Y., et al. 2006, *ApJ*, 650, 57, doi: [10.1086/506376](https://doi.org/10.1086/506376)
- Vayner, A., Wright, S. A., Murray, N., et al. 2021, *arXiv e-prints*, arXiv:2106.08337. <https://arxiv.org/abs/2106.08337>
- Woo, J.-H., Le, H. A. N., Karouzos, M., et al. 2018, *ApJ*, 859, 138, doi: [10.3847/1538-4357/aabf3e](https://doi.org/10.3847/1538-4357/aabf3e)
- Xu, X., Arav, N., Miller, T., & Benn, C. 2018, *ApJ*, 858, 39, doi: [10.3847/1538-4357/aab7ea](https://doi.org/10.3847/1538-4357/aab7ea)
- . 2019, *ApJ*, 876, 105, doi: [10.3847/1538-4357/ab164e](https://doi.org/10.3847/1538-4357/ab164e)
- Xu, X., Arav, N., Miller, T., Kriss, G. A., & Plesha, R. 2020a, *ApJS*, 247, 38, doi: [10.3847/1538-4365/ab596a](https://doi.org/10.3847/1538-4365/ab596a)
- . 2020b, *ApJS*, 247, 42, doi: [10.3847/1538-4365/ab5f68](https://doi.org/10.3847/1538-4365/ab5f68)
- Yuan, F., Yoon, D., Li, Y.-P., et al. 2018, *ApJ*, 857, 121, doi: [10.3847/1538-4357/aab8f8](https://doi.org/10.3847/1538-4357/aab8f8)